UCRL-10788

University of California

Ernest O. Lawrence Radiation Laboratory

IMPACT OF DISLOCATION THEORY ON ENGINEERING

Berkeley, California

DISCLAIMER

UCRL-10788

UNIVERSITY OF CALIFORNIA
Lawrence Radiation Laboratory
Berkeley, California

Contract No. W-7405-eng-48

IMPACT OF DISLOCATION THEORY ON ENGINEERING

John E. Dorn

May 1963

UCRL-10788

IMPACT OF DISLOCATION THEORY

ON

ENGINEERING

by

John E. Dorn[1]

Prepared for Presentation

at the

American Institute of Aeronautics and Astronautics
National Summer Meeting
June 17-22, 1963, Los Angeles, Calif.

[1] Miller Professor of Materials Science 1962-'63, Department of Mineral Technology, University of California; and Research Metallurgist, Inorganic Materials Research Division, Lawrence Radiation Laboratory, University of California, Berkeley, California.

I. INTRODUCTION

Hints concerning the possible importance of some dislocation-like imperfections in crystalline materials were announced in 1928 and 1929 by Prandtl[1] and Dehlinger.[2] In 1934 Taylor,[3] Orowan,[4] and Polanyi[5] independently "invented" models of slip dislocations on which the presently accepted dislocation theory is based.

Progress in extending this new engineering science was extremely slow until after about 1948. Although this delay might in part be attributed to the interruptions occasioned by World War II, it was perhaps principally due to the fact that (1) no one had truly "seen" dislocations except in terms of very indirect evidence, and (2) because several different investigators could marshall evidence to "describe" the same experimental facts in terms of several unique and often apparently contradictory dislocation models. It is now recognized that dislocations are extremely versatile, a fact which stimulates the imagination, and warns against hasty and naive interpretations.

Since 1948 great progress has been made in our grasp of the subject of dislocations: (1) Dislocations can now be "seen" in a number of ways, (2) a vast body of sound theory has already been generated, (3) and a host of experimental observations can now be uniquely and accurately analyzed in terms of the theory. On the other hand the subject is by no means exhausted: Much yet remains to be done before a full and accurate account of all issues can be presented; and because dislocations are so versatile, theory and experiment must yet be advanced simultaneously, each assisting and complementing the other in arriving at the truth.

Your committee suggested that I discuss the "Impact of Dislocation Theory on Engineering," where the title suggests an almost instantaneous

change from a state of quiescence to one of rapid acceleration. In contrast, however, most of the progress has occurred over the past 15 years, albeit at a somewhat exponential rate with time. Because there has been no instantaneous revolutionary change and because dislocation theory is yet evolving, it is indeed difficult to visualize from our present vantage point that any impact might have taken place. Furthermore, each individual advance seems rather small when viewed alone. It is only when dislocation concepts are taken as a whole and comparisons are made over the full increment of the past 15 years that the true nature of the impact is revealed.

Since publications on dislocations are now counted in the tens of thousands, it is physically impossible to review here the full complement of even a small part of the major advances in the area. Therefore, I will confine my discussion to a few issues that might be used to illustrate the possible value of dislocation theory to engineers. Dislocation theory has been, and is currently being, applied toward the development of new alloys: It has already led to the development of non-strain-ageing automotive sheet and to the development of extremely high-strength ausformed steels; it is now being diligently applied to the development of new creep-resistant alloys of the refractory metals and to the possible production of ductile ceramics; numerous other direct engineering applications of dislocation theory are under way. Such direct results of the application of our knowledge about dislocations to engineering are easily appreciated. As I visualize it, however, there is another, perhaps greater, but less obvious significance of dislocation theory to the engineer: It gives him a sound analytical basis in terms of atomistics and the mathematical theory of elasticity on which to base his judgment not only regarding the development of new crystalline materials having special desirable properties but also it gives him the

essential philosophical background to predict how real materials might behave under new and different environmental conditions: It will help him to decide whether or not the plastic behavior of a new material will be temperature or strain-rate sensitive, and whether the flow stress will be so high at low temperatures that notch-sensitivity and brittleness may be imminent; it will provide the basis for formulating the constitutive equations essential to the solution of problems of deformation of engineering materials. In this article I will attempt to illuminate some of these philosophical advantages by a few examples.

Since this paper is being written primarily for those engineers who have at most only a modest background in the subject, I will first review some of the elementary concepts on the nature of dislocations, their stress fields and energies, before approaching some more sophisticated problems. The major issue of the presentation will be the emphasis on the simplicity of the subject.

II. THE NATURE OF DISLOCATIONS

As given in Fig. 1, the theoretical resolved shear stress, τ, for slip in an ideal single crystal is about equal to 1/30 of the shear modulus of elasticity. Whereas extremely small whiskers of metallic and ceramic crystals occasionally approximate this strength, suggesting they are ideal, many pure single crystals begin to deform plastically at 10^{-4} to 10^{-3} of this value, and are therefore imperfect. As shown in Fig. 2, crystals can exhibit point, line or surface imperfections, but the only type of imperfection that can account for slip on a slip plane in a slip direction is the line imperfection known as a dislocation. The unit motion of an edge dislocation is shown in Fig. 3. In contrast to slip in the ideal crystal, Fig. 1, where all atoms on the slip plane move in unison, only small readjustments of atom positions in the vicinity of the core of the dislocation are required to cause slip in the real crystal, Fig. 3. For this reason the yield strength of dislocated crystal can often be quite small. The real crystal, however, can be made quite strong by imposing barriers to the motion of the dislocation, in the form of other dislocations, solute atoms or dispersed particles, etc. Not only do dislocations interact with each other but they also interact with point and surface defects as well.

A general dislocation is shown in Fig. 4 where we have conceived the dislocation to be born at a point of stress concentration so as to sweep out the cross-hatched area. The dislocation line ABCD demarks the region that was displaced by the Burgers vector b in the slip direction from the unslipped portion of the crystal. An extra half plane of atoms was crowded into the region above AB which is now an edge dislocation, as shown in Fig. 2. The edge dislocation line AB is normal to its Burgers vector b, so that the Burgers vector and the line serve to define the slip plane.

MATERIALS: METALLIC AND CERAMIC WHISKERS
(ABOUT 1 MICRON IN DIAMETER)

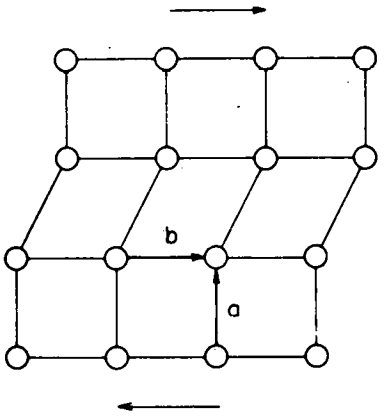

$$\tau_{TH} = \frac{\alpha G b}{2\pi a} \quad (1)$$

τ_{TH} = YIELD STRESS

G = SHEAR MODULUS

$\alpha \simeq \frac{1}{2}$ TO $\frac{1}{3}$

(DEPENDENT ON THE COMPRESSIBILITY OF THE ATOMS.)

MU-30462

Fig. 1. Yield stress in an ideal metal.

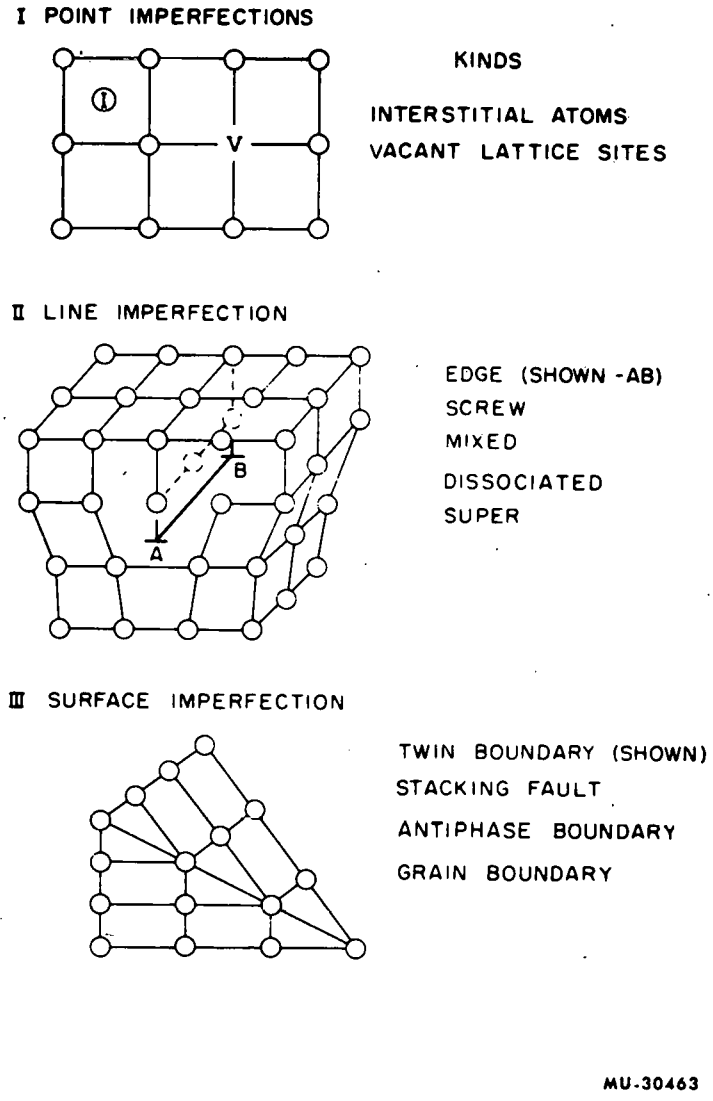

Fig. 2. Crystal imperfections.

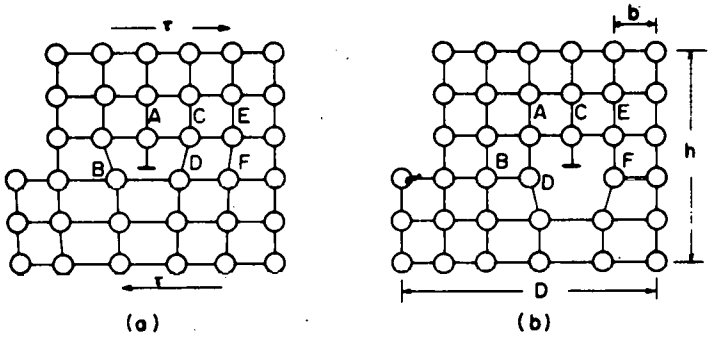

$$\gamma = \frac{b}{h} = \frac{bA}{Ah} = \frac{bA}{V} \qquad (2)$$

$$\dot{\gamma} = \frac{b\dot{A}}{V} = b\rho v \qquad (3)$$

$$\text{WORK} = \tau Ab = F\rho D = FA \qquad (4)$$

$$F = \tau b \qquad (5)$$

γ = SHEAR STRAIN
A = AREA OF SLIP PLANE
V = VOLUME OF CRYSTAL
$\cdot$ = TIME DERIVATIVE
ρ = LENGTH OF DISLOCATIONS PER UNIT VOLUME
F = FORCE OF UNIT LENGTH OF DISLOCATION

MU-30464

Fig. 3. Motion of a dislocation.

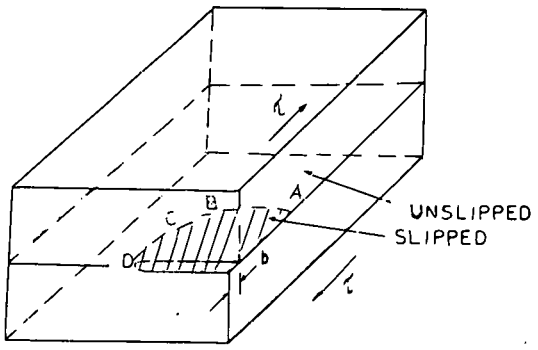

(a) GENERAL SLIP DISLOCATION

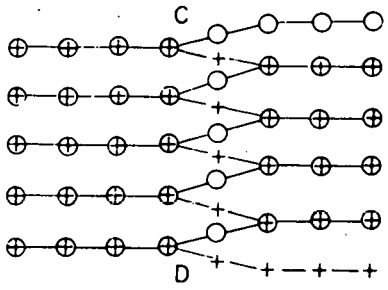

(b) SCREW DISLOCATION, PLAN VIEW OF SLIP PLANE

○ ATOMS ABOVE SLIP PLANE

\+ ATOMS BELOW SLIP PLANE

MU-30465

Fig. 4. General slip dislocation.

Segment CD, shown as a plan view of atomic positions in Fig. 4, is a screw dislocation where the atoms form a spiral ramp about the dislocation line. Since a screw dislocation is parallel to its Burgers vector, this dislocation cannot in general be associated with a specific slip plane. Consequently, pure screw dislocations can cross slip from one plane to another. Segment BC is a mixed dislocation having both edge and screw components. Since slip dislocations are lines that demark slipped from unslipped regions in a crystal, they must either terminate on the surface of the crystal or form closed loops; also the Burgers vector, which is the atomic slip distance, is constant along the total length of a single dislocation.

Dislocations can be "seen" by means of various techniques. Fig. 5, presented through the courtesy of Professor J. Washburn, illustrates a typical three-dimensional Frank network of dislocations as revealed by thin film electron transmission microscopy. Fig. 6 is a deformed and etched single crystal specimen of MgO presented by Professor J. Washburn, showing a series of etch pits at points where dislocations on slip bands intersect the surface of the crystal. Other techniques, including the absorption of infrared light in Si at dislocations decorated with Cu, have been used to "see" dislocations.

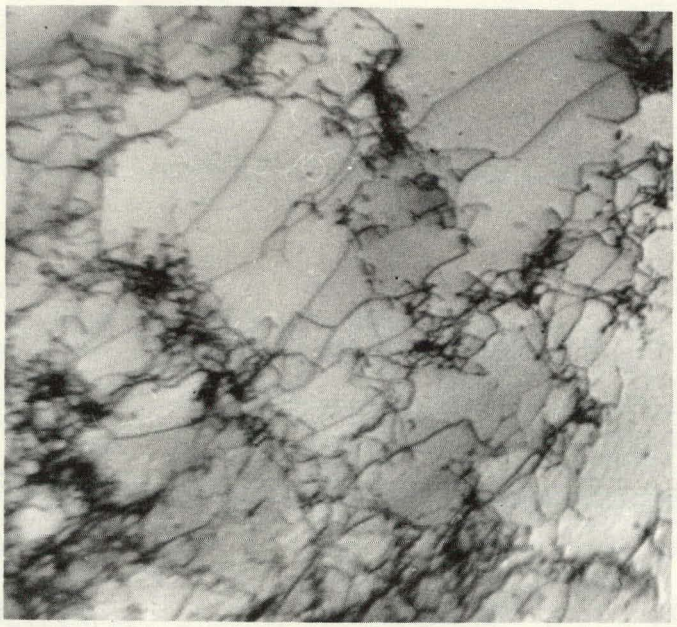

ZN-3697

Fig. 5. Example of transmission electron-micrograph of C_u strained about 10% illustrating the dislocation network and the beginning of the formation of dense entanglements in cells.

By Prof. J. Washburn.

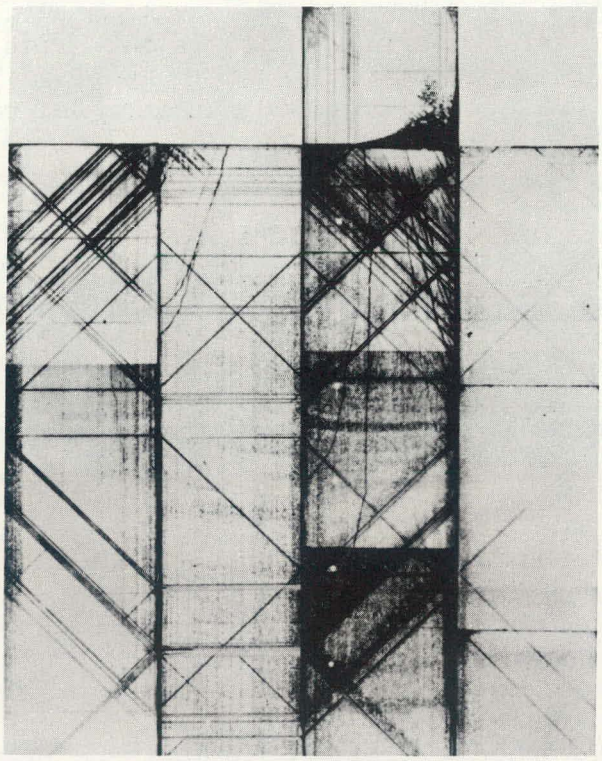

ZN-3698

Fig. 6. Single crystal of M_gO which was strained plastically and etched. Arrays of dislocations can be seen in intersecting slip bands.

By Prof. J. Washburn.

III. STRESS FIELDS AND DISLOCATION ENERGIES

A most interesting feature of dislocation theory arises from the fact that it permits the rationalization of the plastic behavior of crystalline materials in terms of the theory of elasticity. Dislocations, such as CD in Fig. 4b, are the center of a region of elastic deformation in the crystals; and consequently plastic deformation arises only from the motion of such elastic strain centers. Such contained elasticity for continuum mechanics was discussed by several elasticians long before the advent of dislocation theory; for example, important contributions were made as early as 1907 by Volterra[6] in his analyses on "distortioni". Several more pertinent accounts of the mathematical theory for dislocations have now been published.[7-10]

The shear strain γ a distance r from the center of a screw dislocation is readily estimated to be $b/2\pi r$ since the ramp of atoms advances b for one complete circuit.[11] Consequently, the shear stress is $\tau = Gb/2\pi r$. As shown in Fig. 7a, two dislocations of opposite sign on the same slip plane will attract and annihilate each other since the total strain energy is reduced when this happens. When a stress τ is applied, the positive dislocation moves to the right and negative to the left as shown in Fig. 7b. The stress necessary to make them separate must overcome their mutual attractions and therefore exceed $\tau^* = Gb/4\pi y$. Thus as a metal is strained and more dislocations are introduced y decreases, resulting in one of the several contributing mechanisms of strain hardening.

One of the most significant features of a dislocation is its energy;[12] this is the strain energy, Γ_o, induced in the crystal lattice as a result of the dislocation. If we consider a unit length of a screw dislocation, the strain energy per unit volume at a distance r from the core of the dislocation

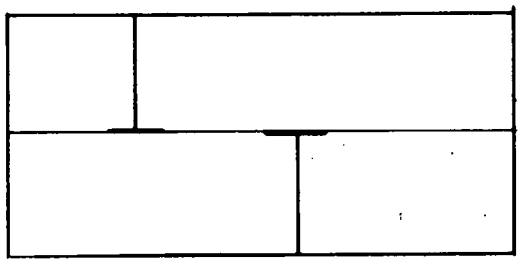

a. TWO DISLOCATIONS ON THE SAME PLANE.

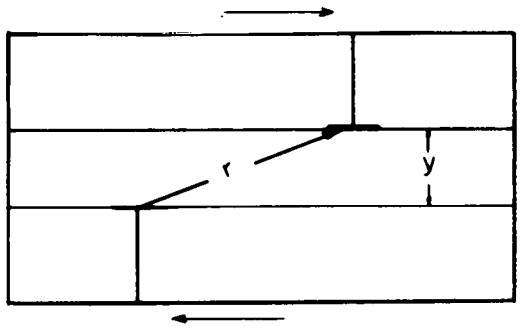

$$\tau_y = \frac{Gb}{4\pi y} \quad (6)$$

b. TWO DISLOCATIONS ON DIFFERENT SLIP PLANES.

MU-30466

Fig. 7. Interaction stresses between dislocations.

is

$$\frac{d\Gamma_o}{2\pi r dr} = \tfrac{1}{2}\tau\gamma = \tfrac{1}{2}\frac{Gb^2}{(2\pi r)^2} \tag{10}$$

For the usual geometric conditions that prevail in establishing the boundary conditions, the integral of the above equation suggests that the energy per unit length of a dislocation is about

$$\Gamma_o = 0.5\,Gb^2 \tag{11}$$

IV. DISLOCATION MECHANISMS

As shown in Table I, the mechanisms that dislocations[13] can undertake are conveniently classified into three major groups:

Table I

Classification of Dislocation Mechanics

Class	Characteristics	Examples
1. Athermal and Velocity Insensitive	Activation energies that are greater than 50kT, therefore cannot be thermally activated. Deformation stresses that are independent of the strain rate and insensitive to the test temperature. Usually $\tau = \tau\{\gamma^e\}$ (12)	1A. Long-range stress fields 1B. Short-range and long-range ordering in alpha solid solutions. 1C. Suzuki-locked alloys.
2. Thermally Activated	Activation energies that are less than 50kT. Flow stresses that decrease rapidly with an increase in temperature or a decrease in strain rate. Creep processes. $\dot{\gamma} = f^+\{\tau, str, T\}e^{-\frac{U^+\{\tau, str, T\}}{kT}} - f^-\{\tau, str, T\}e^{-\frac{U^-\{\tau, str, T\}}{kT}}$ (13)	2A. Peierls process 2B. Intersection 2C. Cross slip for dissociated dislocations 2D. Motion of jogged screw dislocations 2E. Climb of edge dislocations 2F. Viscous creep due to solute atom interactions
3. Athermal but Velocity Sensitive	Not thermally activated but yet exhibiting an effect of strain rate on the stress.	3A. Relativistic motion of dislocations,[15] 3B. Phonon interactions with moving dislocations.[16] $\dot{\gamma} = \frac{10}{3}\frac{\rho b^4 c \tau}{kT}$

Occassionally only one of these mechanisms controls the plastic deformation. More frequently, however, several are operative at one time. As shown by Eqn. 12, the athermal processes have flow stresses that are independent of the strain rates. In contrast thermally activated processes exhibit flow stresses that decrease with increasing temperatures and decreasing strain rates.[14] In Eqn. 13, f^+ is the frequency and u^+ is the activation energy for the forward motion of dislocations. The amount of energy u^+ that must be supplied by a thermal fluctuation in order to activate the process depends strongly on the applied stress, τ, usually u^+ also depends on the dislocation substructure, str, and only mildly on the temperature, T. The net strain rate is obtained by taking the difference between the forward (+) and the reverse (-) rates.

In the following discussion some of the details of several examples of dislocation mechanisms will be reviewed.

V. SUZUKI LOCKING OF DISLOCATIONS

Suzuki solute atom locking of dislocations is an interesting example of athermal process.[17] The atomic arrangements of atoms on successive (111) planes in FCC crystals, as shown in Fig. 8, follow the sequence ABCABC - -. The total slip or Burgers vector is b, the closest distance between identical atoms in the slip direction. The total Burgers vector b, however, will dissociate into a pair of Shockley partials as shown by the "chemical" Eqn. (a), because the total energy decreases for this reaction as calculated in Eqn. (b). When this dissociation occurs as a result of a dislocation between the A and B planes, the new arrangement in Fig. 9 is obtained. The two Shockley partials are A A' having a Burgers vector b, and B B' having a Burgers vector b_2. Whereas to the left of A A' and to the right of B B' the atoms have the normal sequence of layering for the FCC system, between the two Shockley partials they have the sequence -- C|AC|ABC-- and thus exhibit a stacking fault. Since the sequence - - - C A C A C A - - is that for the layering of successive basal planes in the hexagonal CP system, the stacking fault consists of two layers of atoms based on the hexagonal scheme. Since the FCC system is the more stable, the free energy of the crystal increases as the partials separate to greater distances. A minimum total free energy change is encountered at an equilibrium distance of separation d. An analogous situation occurs on the basal plane of hexagonal CP metals, where now the stacking fault consists of two layers of atoms arranged in the FCC sequence.

Suzuki illustrated that when a binary alloy is at sufficiently high temperature, e.g. above about 0.4 of the melting temperature, so that diffusion can occur, the solute element will distribute itself between the surrounding ideal crystal and the stacking fault as demanded in all two component-two phase

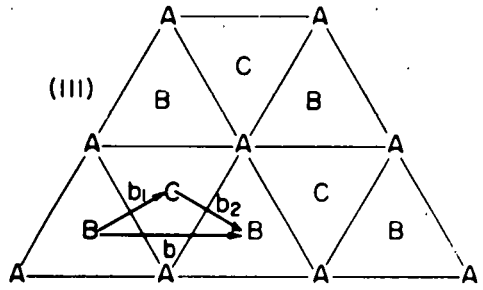

$$(a)\quad \mathbf{b} \longrightarrow \mathbf{b}_1 + \mathbf{b}_2 \tag{14}$$

$$(b)\quad \Delta U \cong \frac{G}{2}\left(\bar{b}_1 \cdot \bar{b}_1 + \bar{b}_2 \cdot \bar{b}_2 - \bar{b} \cdot \bar{b}\right) = \frac{Ga^2}{2}\left(\frac{6}{36} + \frac{6}{36} - \frac{2}{4}\right) = \frac{-Ga^2}{12} \tag{15}$$

MU-30467

Fig. 8. Atomic arrangement and Burgers vectors in FCC crystals.

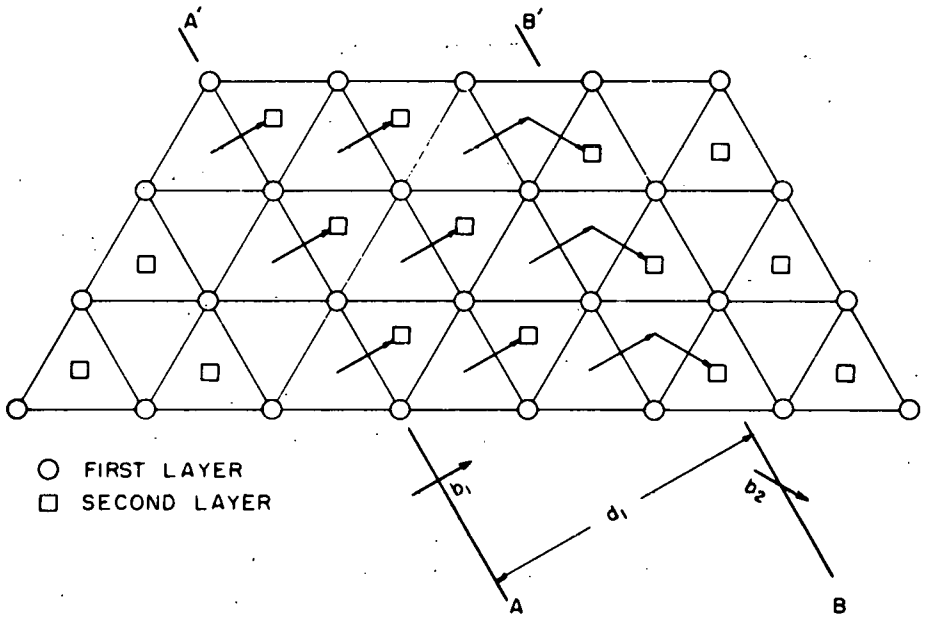

Fig. 9. Partially dissociated dislocation.

equilibria. Under these conditions the situation shown in Fig. 10 will prevail. A composition c_f of the solute atoms will be obtained in the stacking fault whereas the composition in the sound part of the crystal will remain nearly the average composition c. If a unit length of each partial dislocation is moved a distance δ by an applied stress τ, the work done is $\tau b \delta$, as we have described earlier. In doing this work the volume $2h\delta$ is swept out by each partial dislocation, where h is the height of each atomic layer. As dislocation A moves to A' the increase in free energy is $\frac{2h}{V}\left(F_{c_f} - F^f_{c_f}\right)$ where V is the molar volume, F_{c_f} and $F^f_{c_f}$ are the free energies at composition c_f of the ideal crystal and the fault respectively. Similarly the motion of the partial dislocation from B to B' requires an increase in free energy of $\frac{2h}{V}(F^f_c - F_c)$. Since the work done by the stress mechanically must account for the total increase in chemical free energy

$$\tau = \frac{2h}{V}\left\{\left(F^f_c - F_c\right) - \left(F^f_{c_f} - F_c\right)\right\} \tag{16}$$

where $2h/bV$ is well known from the crystal structure. The necessary thermodynamic data for obtaining the equilibrium composition c_f and the free energies F^f_c and $F^f_{c_f}$ in the faulted region are not known so that the deformation stress τ cannot yet be accurately calculated. Assuming, however, that both the ideal crystal and the faulted region are ideal solutions, it follows that under equilibrium conditions

$$\frac{c_f}{1-c_f} = \frac{c}{1-c} e^{-\frac{\Delta F}{kT}} \tag{17}$$

where

$$\Delta F = \left\{\left(F^f_c - F_c\right) - \left(F^f_{c_f} - F_{c_f}\right)\right\} = \frac{V}{2h}\left(\gamma_b - \gamma_a\right) \tag{18}$$

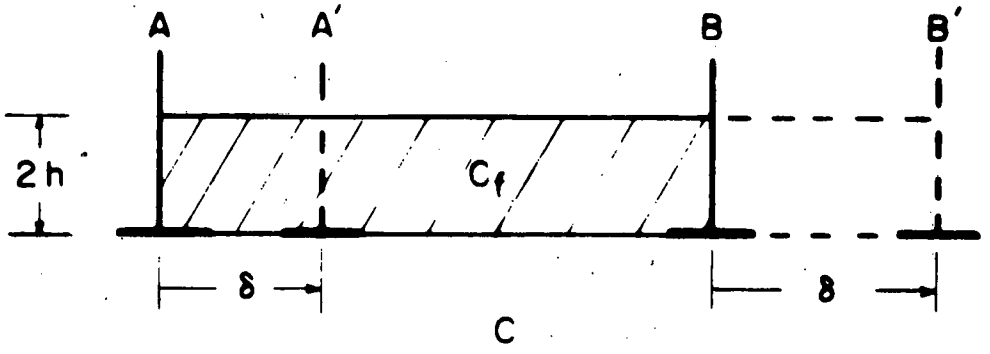

MU-30469

Fig. 10. Movement of dislocations in Suzuki locked alloy.

and where γ^e_b and γ^e_a are the stacking fault energies per cm^2 in the pure components b and a of the alloy. In this event

$$\tau = \frac{1}{b}(c - c_f)(\gamma^e_b - \gamma^e_a) \tag{19}$$

The work that must be done to unlock a Suzuki locked alloy can be quite high and it cannot be supplemented by local thermal fluctuations. Therefore the deformation stress changes as a result of a change in temperature only insofar as the temperature affects $\gamma^e_b - \gamma^e_a$. Suzuki locked alloys, therefore, can maintain rather high flow stresses even up to temperatures approaching their melting temperature. The introduction of Suzuki locking might provide one of the bases for the development of engineering alloys that can maintain their strengths even at high temperatures.

Up to the present only one unique example of effective Suzuki locking has been uncovered. The resolved shear stress-strain curve for basal slip in the hexagonal phase of Ag containing 33 atomic percent Al is shown in Fig. 11. At the upper yield point a single Luder's band having a Luder's strain of 1.35 is produced which migrates over the gage length of the specimen; after this only a modest amount of strain hardening is exhibited. The upper and lower yields strengths as a function of temperature and strain rate are shown in Fig. 12. It is immediately apparent that changes in the shear strain rates from 10^{-4} to 10^{4} per second do not materially affect the yield strength. Furthermore, in contrast to the usual trends, the upper yield strength increases as the temperature increases above about 0.4 of the melting temperature. These trends are wholly inconsistent with those obtained as a result of Cottrell pinning of dislocations and are consistent only with the trends expected in Suzuki locked alloys. Assuming that Suzuki locking is operative,

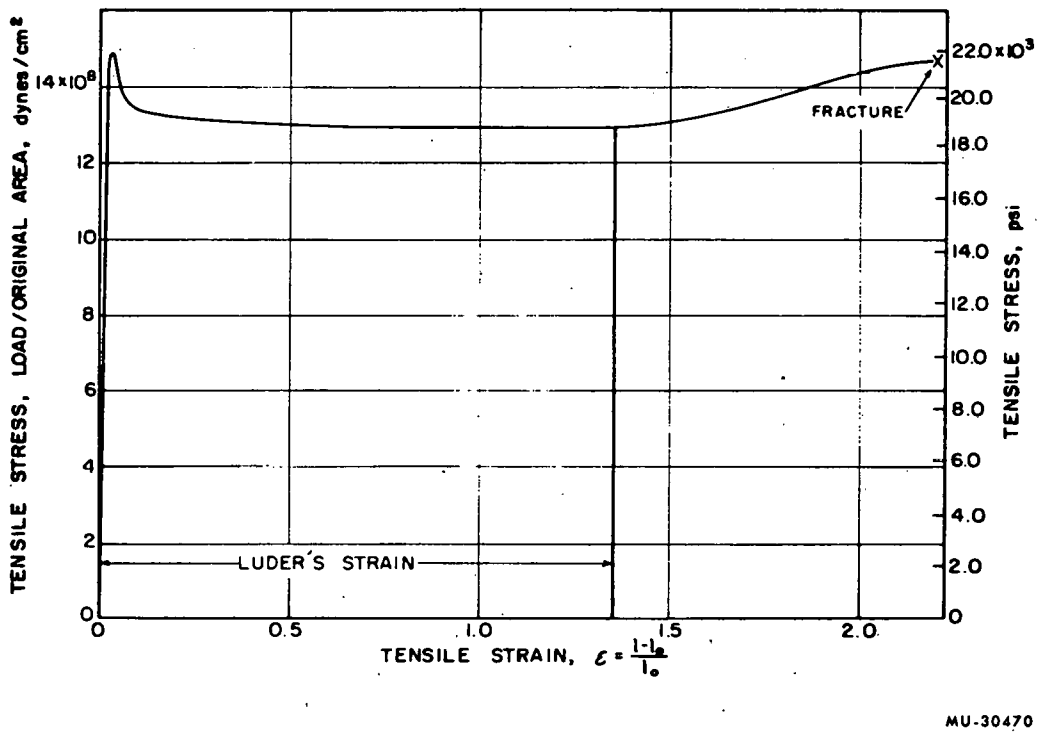

Fig. 11. Tensile stress-tensile strain diagram for basal slip.

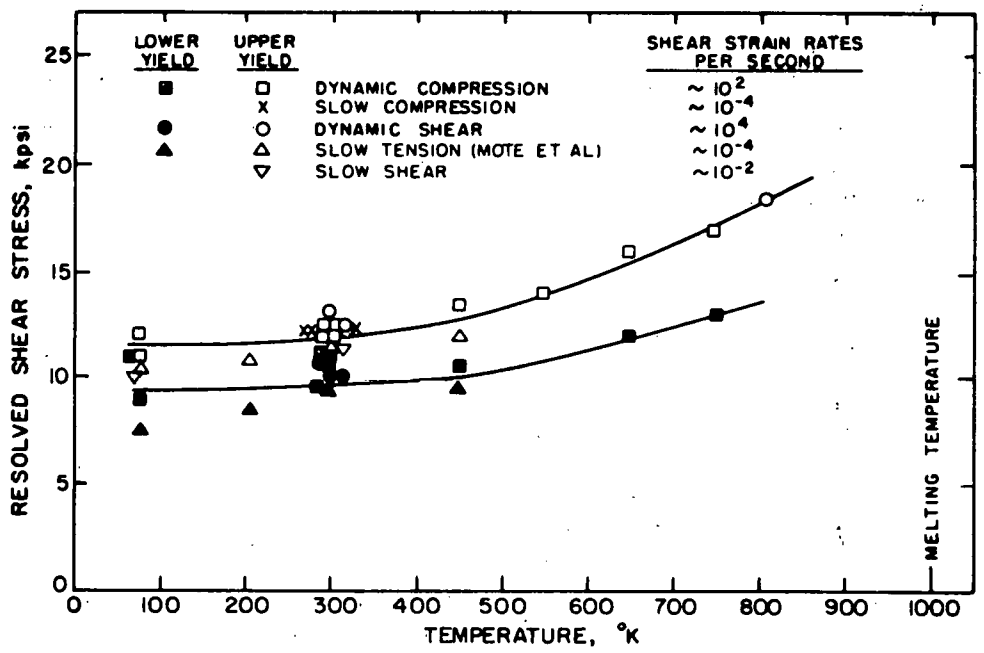

MU-30471

Fig. 12. Resolved shear stress vs. temperature for basal slip.

the values of $\gamma^e_b - \gamma^e_a$ as deduced from the experimentally determined upper yield strength is shown in Fig. 13, the analysis being made only over the higher temperature range where equilibrium is expected to be maintained. The negative set of values can be shown to be applicable; they are not higher than what are estimated to be reasonable values for stacking fault energies and their almost linear variation with temperature is expected. There can be little doubt that the high temperature resistance to basal slip in this alloy is due to Suzuki locking.

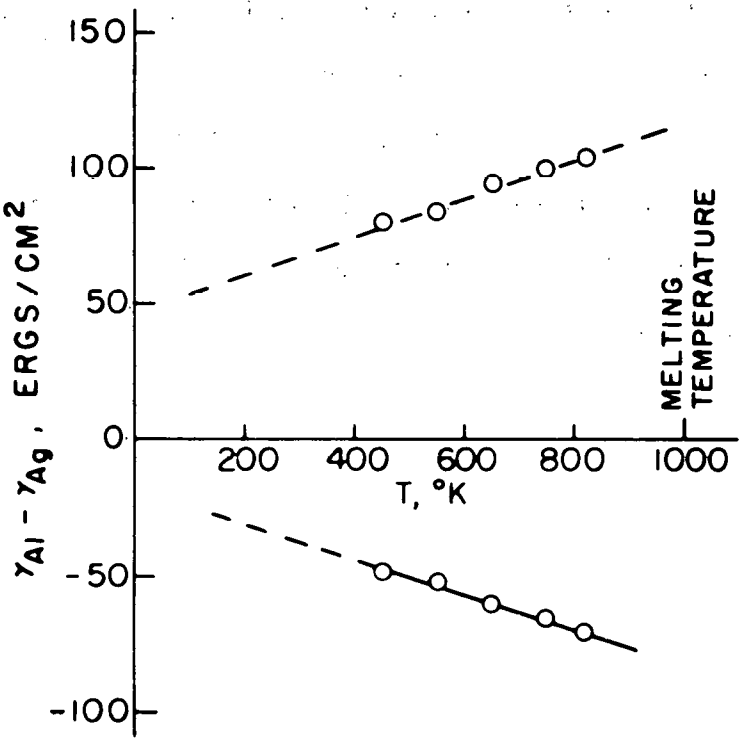

Fig. 13. Stacking fault energies vs. temperature.

VI. THE PEIERLS MECHANISM

The Peierls mechanism, which is strain rate controlling for the low temperature plastic flow of the refractory BCC metals and for prismatic slip in hexagonal CP metals, will be used to illustrate a thermally activated mechanism. This mechanism has been discussed by Seeger,[18] Seeger, Donth and Pfaff,[19] Lothe and Hirth,[20] and Friedel.[21] I will present here, however, a brief outline of a more recent and more accurate analysis by Dorn and Rajnak.[22]

A dislocation has its lowest energy when it lies in a valley parallel to a line of closely packed atoms as shown in Figs. 3a and 3b. As the dislocation moves from 3a to 3b, the bond angles and distances between the atoms change resulting in an increase in energy. Whereas in FCC metals this increase is extremely small, it becomes appreciable in BCC metals which probably exhibit some covalent bonding. Although more general cases have been explored by Dorn and Rajnak, I will assume here that the Peierls hill is sinusoidal as shown in Fig. 14, in terms of the line energies per unit length of a dislocation, Γ_c and Γ_o at Peierls hilltop and valley respectively. In order to move the dislocation en mass over the Peierls hill at the absolute zero it requires a Peierls stress, τ_p, where the maximum force per unit length of the dislocation is

$$\tau_p b = \left(\frac{d\Gamma}{dy}\right)_{y/a=\pi/2} = \frac{\pi}{a}(\Gamma_c - \Gamma_o) \qquad (22)$$

When stress $\tau < \tau_p$ is applied, the dislocation will advance part way up the Peierls hill to a position y_o, as shown in Fig. 15, where

$$\tau b = \left(\frac{d\Gamma}{dy}\right)_{y_o} = -\frac{\pi}{a}(\Gamma_c - \Gamma_o)\sin\frac{2\pi y_o}{a}$$

$$= -\tau_p b \sin\frac{2\pi y_o}{a} \qquad (23)$$

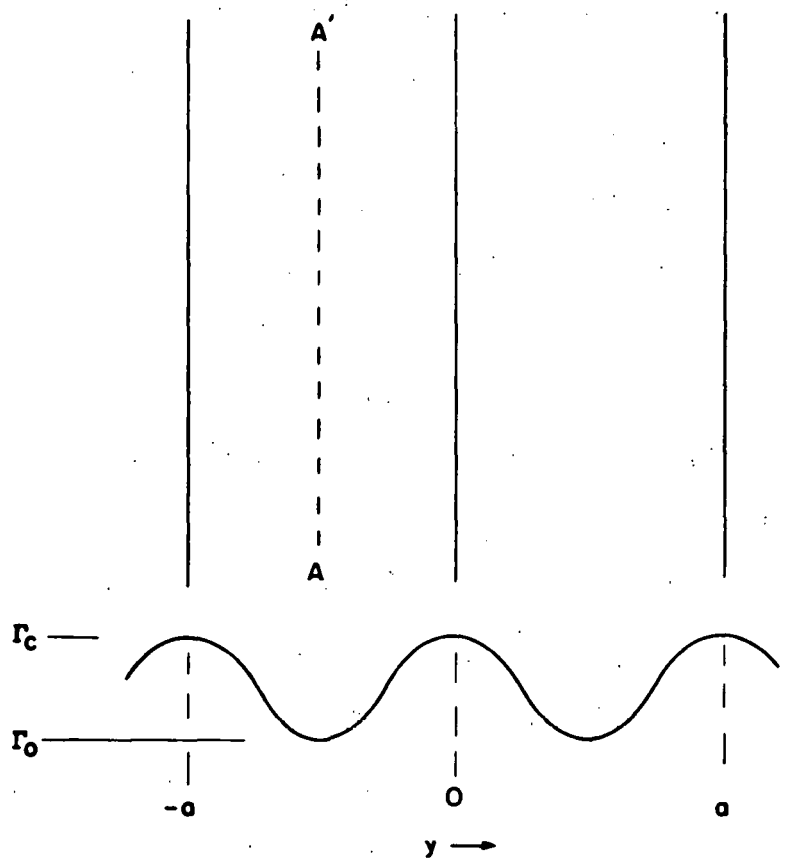

$$\Gamma = \frac{\Gamma_c + \Gamma_o}{2} + \frac{\Gamma_c - \Gamma_o}{2} \cos 2\pi y/a \qquad (20)$$

$$\Gamma \simeq Gb^2/2 \qquad (21)$$

MU-30473

Fig. 14. Peierls hills and a dislocation AA' lying in the valley.

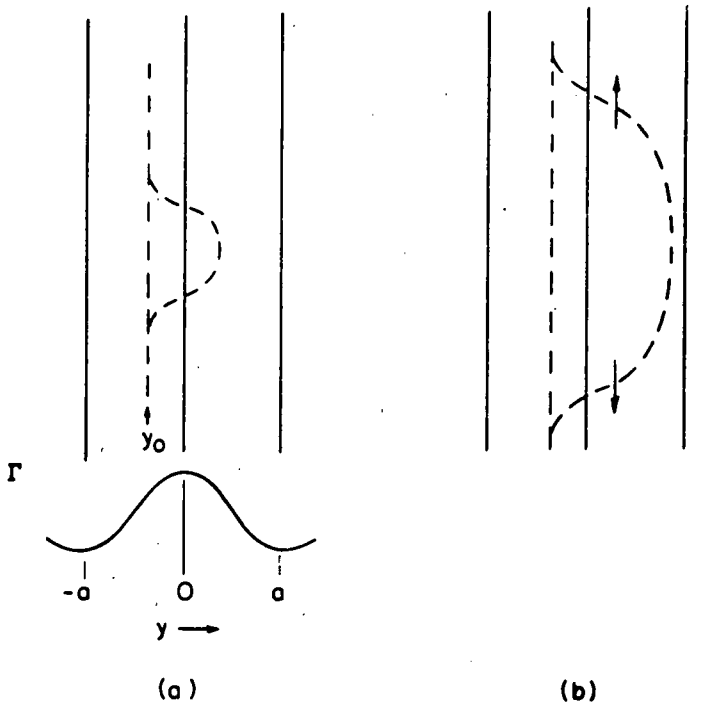

Fig. 15. The nucleation of a pair of kinks.

At temperatures above the absolute zero, thermal fluctuations can assist the stress to locally bow out the dislocation as shown in Fig. 15a. When the energy of the thermal fluctuation is great enough a pair of kinks will be produced as shown in Fig. 15b; such kinks will then migrate under the applied stress to the geometric limits of the dislocation segment on which they formed. The frequency of nucleation of the pair of kinks ν_n in a length L is given by the Boltzmann condition, namely

$$\nu_n = \frac{L}{w} \nu_D e^{-\frac{u_n}{kT}} \tag{24}$$

Where u_n is the saddle point energy required to form two kinks, k is the Boltzmann constant, T is the absolute temperature, ν_D the Debye frequency, L the length of the dislocation, and w is about the length over which the critical fluctuation takes place. Then, in accord with our previous discussions, the shear strain rate for the Peierls mechanism will be given by

$$\dot{\gamma} = \rho/L (L a) \frac{L}{w} \nu_D e^{-\frac{u_n}{kT}} \tag{25}$$

Where ρ is the total length of dislocations per cm^3, ρ/L is therefore the number of lengths L, and La is the area swept out per successful fluctuation. The above formulation of the Peierls mechanism is valid so long as only one pair of kinks are moving at one time in each segment of a dislocation. Dorn and Rajnak have also formulated the Peierls process when many pairs of kinks are formed in the same length L. Neglecting the effect of stress on w because this is not significant, reveals that to a high degree of accuracy the stress affects the strain rate principally as a result of its effect on u_n.

The value of u_n is equal to the increase in the dislocation line energy when the dislocation acquires the critical configuration for the nucleation of a pair of kinks. For any shape of dislocation this is

$$u = \int_{-\infty}^{\infty} \left[\Gamma\{y\} \sqrt{1 + \left(\frac{dx}{dy}\right)^2} - \Gamma\{y_o\} - \tau b (y - y_o) \right] dx \tag{26}$$

Where the first term gives the line energy of the dislocation moved so that it has the shape $y \equiv y\{x\}$, the second term Γ_{yo} gives the line energy when the dislocation is in its equilibrium position at $y = y_o$ under the stress, τ, and $\tau b\,(y - y_o)$ gives the work done by the stress during the displacement of the dislocation line from y_o to $y \equiv y\{x\}$. The least energy to produce a pair of kinks is evaluated by displacing the dislocation line so that it will pass through $\lambda = y$ at $x = 0$ as shown in Fig. 16. As λ first increases above y_o the line length increases resulting in an increase in energy. The static equilibrium shape of the dislocation line for all values of $y \leq \lambda \leq \lambda_c$ is well defined and easily determined as will be shown. Beyond λ_c, at which point $\left(\frac{dy}{dx}\right)_{x=o} = 0$, static equilibrium cannot be obtained. The above integral for u, when the dislocation passes through λ_c gives the saddle point energy, u_n, for the nucleation of a pair of kinks.

The condition of equilibrium for any curve going through $x = 0$ and $y = \lambda$ is determined by minimizing the energy given by Eqn. 26. This condition is determined in terms of the calculus of variations by Euler's equation, that

$$\frac{\partial}{\partial y}\left[\Gamma\{y\}\sqrt{1+\left(\frac{dy}{dx}\right)^2} - \Gamma_o\{y_o\} - \tau b (y - y_o)\right] =$$

$$\frac{d}{dx}\frac{\partial}{\partial\left(\frac{dy}{dx}\right)}\left[\Gamma\{y\}\sqrt{1+\left(\frac{dy}{dx}\right)^2} - \Gamma\{y_o\} - \tau b (y - y_o)\right] \tag{27}$$

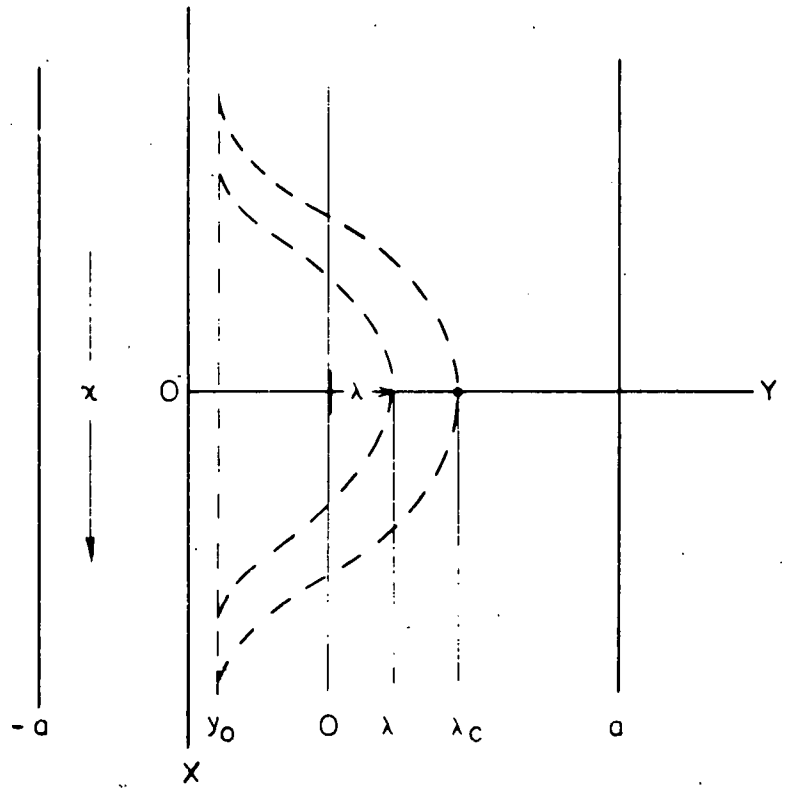

MU-30475

Fig. 16. Configurations during the nucleation of a pair of kinks.

$$\tau_b = \frac{d}{dy}\left[\frac{\Gamma\{y\}}{\sqrt{1+\left(\frac{dy}{dx}\right)^2}}\right] \tag{28}$$

Upon integration once and the substitution of appropriate boundary conditions Eqn. 28 gives

$$\frac{dy}{dx} = \pm\sqrt{\frac{\Gamma^2\{y\} - \left[\Gamma\{y_o\} + \tau_b(y-y_o)\right]}{\left[\Gamma\{y_o\} + \tau_b(y-y_o)\right]^2}} \tag{29}$$

At $y = \lambda_c$, the two slopes at $x = 0$ become equal to zero, which requires that

$$\Gamma\{\lambda_c\} = \Gamma\{y_o\} - \tau_b\{\lambda_c - y_o\} \tag{30}$$

Changing the independent variable of Eqn. 26 from x to y, and introducing the equilibrium condition given by Eqn. 29 reveals that

$$u_n = 2\int_{y_o}^{\lambda_c}\sqrt{\Gamma^2\{y\} - \left[\tau_b(y-y_o) + \Gamma\{y_o\}\right]^2}\,dy \tag{31}$$

Where λ_c is defined by Eqn. 30. When the stress, τ, is zero $u_n = 2u_k$, where u_k is the energy of a single isolated kink. Numerical integration of Eqn. 31 is given in Fig. 17.

Although the theory has been developed in much greater detail, only a few correlations can be given here: As shown by Eqn. 25, for a constant strain rate test, u_n increases linearly with the absolute temperature. At the absolute zero, u_n is zero and as shown in Fig. 17 $\tau = \tau_p$. As the temperature of the test increases, u_n increases and τ correspondingly decreases

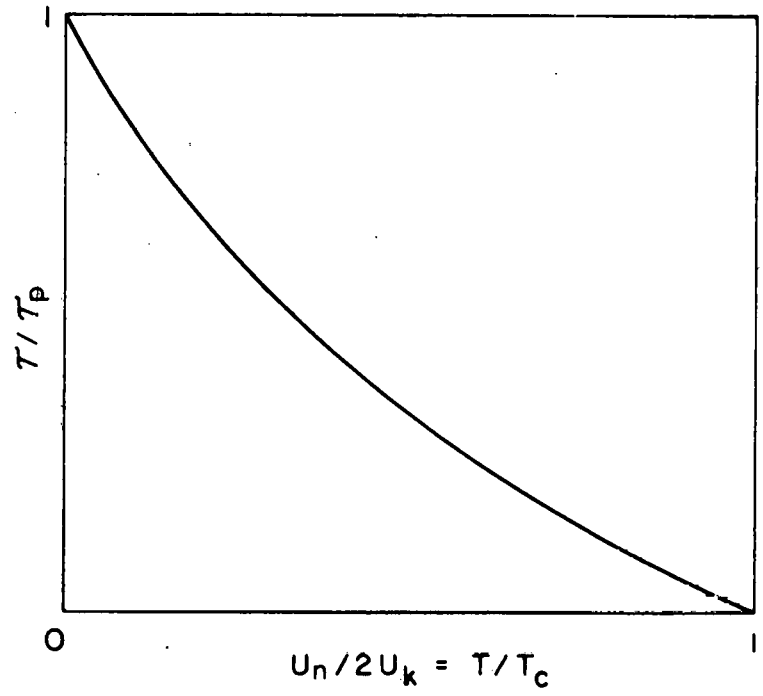

MU-30476

Fig. 17. Effect of stress on the energy to nucleate a pair of kinks.

as illustrated in Fig. 17. At some critical temperature, T_c, $u_n = 2u_k$ and $\tau = 0$. Equation 25 is therefore valid from $0 \leq T \leq T_c$ where

$$\dot{\gamma} = \rho/L\,(La)\,b\,\frac{L}{\omega}\,\nu_D\,e^{-\frac{2u_k}{kT}} \tag{32}$$

Within this range of temperatures, as seen by comparing Eqn. 25 and 32,

$$\frac{u_n}{2u_k} = \frac{T}{T_c} \tag{33}$$

Therefore, for the idealized Peierls mechanism where the Peierls hill is approximately sinusoidal and where only one pair of kinks is formed in length L of a dislocation and auxiliary solute atom effects on the nucleation and migration of a pair of kinks is small, the flow stress should vary with the temperature as shown in Fig. 17. If τ_a is the applied shear stress and τ^* is due to overcoming athermal mechanisms, τ must be associated with $\tau_a - \tau^*$. The datum points of Fig. 18 represent experimental values whereas the curves through the points are the theoretical predictions deduced from Fig. 17. The excellent agreement between theory and experiment attests to the fact that the Peierls mechanism is operative in these metals and alloys.

Many important details concerning the low temperature plastic behavior of the refractory BCC metals can now be correlated in terms of the theory. Unfortunately these cannot be discussed here because of limitations of space; a very few will be briefly mentioned. For example, the almost horizontal portion of the experimental data for W as the temperature approaches zero represents not plastic flow but fracturing. As shown by Eqn. 32, a decrease in $\dot{\gamma}$ or an increase in ρ would result in a lower value of T_c and therefore a higher temperature for the transition from the brittle to ductile behavior.

The value of ρ might be increased by small plastic deformations in the ductile region introducing thereby many unlocked dislocations. Increased localized strain rate due to the presence of notches will result in higher flow stresses and increased danger of notch brittleness, Metals having higher shear moduli and higher Peierls hills will be more susceptible to low temperature brittleness. Since the flow stress can now be analyzed in terms of the Peierls theory, half of the theory for brittle fracturing is known; the remaining part concerns the effect of various factors on the fracture stress.

VII. PLASTIC WAVES

As another example of the impact of dislocation theory on engineering, I should like to illustrate very briefly some implications of dislocation theory to the problem of plastic wave propagation. All mathematical theories for plastic wave propagation, which are extensions of the classical theory developed independently by von Karman[23] and Taylor,[24] are based on the equations for conservation of momentum and on the conditions for continuity. For the simple case of a plastic wave moving down a very thin rod, these equations are as follows:

	Continous Variations		Hugoniot Shock Conditions	
Condition for Continuity	$\frac{\partial \epsilon}{\partial t} = \frac{\partial v}{\partial \alpha}$	(34a)	$[\epsilon]\frac{d\alpha}{dt} = -[v]$	(34b)
Conservation of Momentum	$\frac{\partial \sigma}{\partial \alpha} = \rho \frac{\partial v}{\partial t}$	(35a)	$[\sigma] = -\rho[v]\frac{d\alpha}{dt}$	(35b)

where

ϵ = the axial engineering strain

t = time

v = particle velocity

α = the Lagrangian coordinate along the axis of the rod

σ = the axial engineering stress

ρ = the density

[ ] = a shock in the bracketed value

Equations 34b and 35b reveal that the velocity of a shock along the rod is

$$\frac{d\alpha}{dt} = \sqrt{\frac{1}{\rho}\frac{[\sigma]}{[\epsilon]}} \qquad (36)$$

Since there are three dependent variables (σ, ε, and v) Eqns. 34 and 35 must be solved simultaneously with a third equation which describes the plastic behavior of the material of which the rod is made. In their outstanding classical development of the theory, von Karman and Taylor assumed that the deformation stress is always exclusively a function of the strain according to $\sigma \equiv \sigma(\varepsilon)$. Dissecting a finite shock into a series of small shocks such that $[\sigma]/[\varepsilon]$ for each small shock approximates $d\sigma/d\varepsilon$, the velocity of the shock becomes

$$\frac{\partial \alpha}{\partial t} = \sqrt{\frac{d\sigma/d\varepsilon}{\rho}} \tag{37}$$

Therefore, the velocity of elastic waves at stress levels below the yield strength is equal to $\sqrt{E/\rho}$ where E is Young's modulus, whereas plastic waves are predicted to travel at slower velocities since $d\sigma/d\varepsilon$ is less then E in the plastic region.

The only debatable issue in the original formulation of the theory for plastic wave propagation concerns the assumption that the deformation stress is exclusively a function of the strain, independent of any time effects. The answer to this question for plastic waves in crystalline materials must be sought in terms of the behavior of dislocations.

Frank[25] has shown that the line energy per unit length of a dislocation increases with its velocity. For a screw dislocation moving with a velocity, v, the line energy Γ_v is given by the relativistic-like equation

$$\Gamma_v = \Gamma_o \Big/ \left\{1 - \left(\frac{v}{c}\right)^2\right\}^{1/2} \tag{38}$$

where Γ_o is the rest energy of the dislocation and c is the velocity of an

elastic shear wave in the crystal. Several important deductions result: The energy of a dislocation becomes infinite as its velocity approaches the speed of sound. Unless certain special conditions prevail, a dislocation cannot have a velocity that exceeds the speed of sound. Dislocations have inertia. For example, expanding Eqn. 38 into a Taylor's series reveals that the effective mass of a slow moving dislocation is Γ_o/c^2.

When a stationary dislocation is subjected to a shock in stress, it will immediately begin to accelerate; but since it has inertia, the shock in stress cannot cause an instantaneous displacement of the dislocation. Therefore, no shock in plastic strain is possible; the shock in the total strain being exclusively a shock in elastic strain. Therefore, Eqn. 37 is in general invalid and, as shown by Eqn. 36, the shock in strain being only the shock in elastic strain, the wave will travel down the bar with the speed of an elastic wave. This deduction is consistent with the experimental facts deduced by Sternglass and Stewart,[26] Alter and Curtis,[27] and Riparbelli.[28]

The fact that dislocations have inertia suggests that under shock loading it will be necessary to account for the acceleration of dislocations by expressing the rate of change of strain rate in terms of the applied stress. Neglecting velocity sensitive dissipative mechanisms, the accelerative period can be estimated by equating the rate at which work is done on the dislocation to the rate of increase of line energy of the moving dislocation. Accordingly,

$$(\tau - \tau^*) b v = \frac{d\Gamma}{dt} \tag{39}$$

where τ^* is the stress at which dislocations will first move against

long-range stress fields. Integrating Eqn. 39, letting $v = 0$ at $t = 0$ gives

$$(\tau - \tau^*) bct = \frac{\Gamma_o}{c^2} \frac{v}{\sqrt{1-(\frac{v}{c})^2}} \tag{40}$$

Consequently introducing the values appropriate for Al, namely $c = 5 \times 10^5$ cm/sec, $b = 2.86 \times 10^{-8}$ cm, and $\Gamma_o \simeq Gb^2/_2 = 1.1 \times 10^{-4}$ ergs/cm, the dislocation will achieve a velocity of 0.9C in 2×10^{-11} sec, for the small stress of 10^8 dynes/cm^2. Obviously, the inertia of a dislocation is so small that it accelerates to its limiting velocity in an extremely brief period of time. The shear strain at this time is given by

$$\gamma = \int_0^{2\times10^{-11}} \rho b v \, dt = 1.4 \times 10^{-4} \tag{41}$$

where ρ the density of moving dislocations was taken to be 10^8/cm^2. Therefore, the plastic strain to be expected over the accelerative period of dislocation motion is also extremely small. Consequently, the formulation of the dynamic plastic behavior of crystalline materials need take into consideration rates of change of strain rates only when information is needed for times less than about 10^{-11} sec, and for plastic strains of less than about 10^{-4}.

For most analyses on plastic wave propagation, interest centers about longer times and larger plastic strains than those which occur during the period that dislocations might be accelerating. Consequently, time need not be considered to the second order in terms of $\frac{d^2\gamma}{dt^2}$ but only to the first order in terms of $d\gamma/dt$. Some dislocation processes that depend on time to the first order of magnitude are listed under items two and three of Table I. A typical example of the large effects of strain rate on the flow

stress is illustrated in Fig. 18.[29-33] The data for slow strain-rate tests reveal three regions. Whereas the thermally activated Peierls process is operative over Region I, the athermal short-range order mechanism controls the flow stress over Region II, and a thermally activated diffusion process is strain-rate controlling over Region III. Under dynamic testing, however, T_c, for the upper temperature limit of the Peierls mechanism is shifted, in agreement with theory, to much higher temperatures. Furthermore, the times are so short under dynamic test conditions that no plastic straining can result from the diffusion-controlled mechanism. Consequently, under sufficiently high strain rates only the Peierls mechanism operates in this example. At 600°K the yield stress for the high strain rate tests is at least fifteen times greater than those for the low strain rates illustrating the significant changes in deformation mechanisms that are introduced as a result of dynamic test conditions.

The von Karman assumption that $\sigma \equiv \sigma(\epsilon)$ is useful only in a few cases where dislocation processes are insensitive to the strain rate. Examples of these processes are given in section 1 of Table I. A typical example, due to short-range ordering, is shown in Region II of Fig. 18. As previously discussed, however, such athermal strain rate insensitive processes are usually accompanied by low temperature thermally activated mechanisms. And the temperature range over which such thermally activated mechanisms operate is increased as the strain rate is increased. Consequently, as shown in Fig. 18, the athermal and strain-rate insensitive mechanism operative over Region II is replaced by the lower temperature, thermally activated and strain-rate sensitive mechanism that was only operative over Region I under slow strain rates. If, however, no such thermally activated mechanisms are operative at the lower temperatures, as shown by the example given in

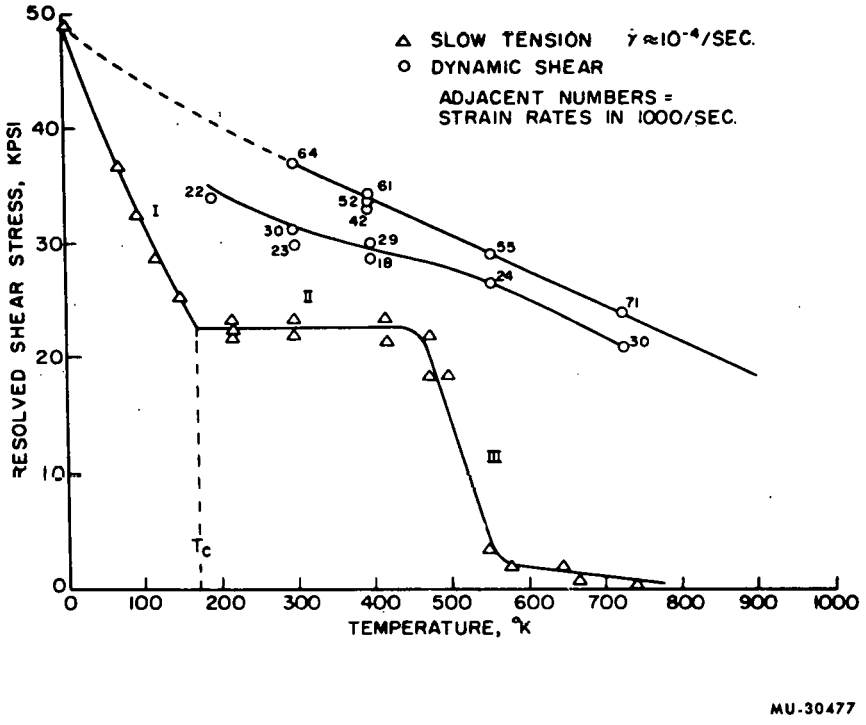

Fig. 18. Prismatic yielding of an Ag(67%)-Al(33%) alloy.

Fig. 12, the plastic behavior remains athermal and insensitive to strain rates for all conditions of test. Only when these stringent conditions are met is the von Karman assumption that $\sigma \equiv \sigma(\varepsilon)$ a reasonable approximation to the facts. For all other cases the strain-rate sensitive theories of plastic wave propagation should be employed.

VIII. SUMMARY

Whereas dislocation concepts and theory are now being employed in considerable depth toward the development of new and better engineering alloys, the great impact of dislocation theory on engineering has resulted principally from the correlated and unified philosophical approach it has given engineers toward the understanding of the mechanical behavior of materials. The author has attempted to set forth several recent items of research progress of special personal interest in order to illustrate how dislocation theory works and what it can do. He hopes that in doing so he has shown that dislocations permit a description of plastic behavior in terms of the motion of lines of elastic discontinuities in crystals. Thus, dislocation theory is, in some respects, only a modest extension of the elasticity theory that is so familiar to engineers.

It appears that any engineer whose work impinges upon the behavior of materials is now seriously handicapped if he does not have at least a modest background in dislocation theory. When the few examples of deductions and correlations of mechanical behavior, given in the text of this report, are supplemented with the full scope of the application of dislocation theory to engineering, the great utility of the theory to many types of problems becomes ever more apparent and urgent.

As must be evident from the context of this report, dislocation theory need not be extremely esoteric or complex. Every engineer has the essential mathematical, physical and chemical background to understand and become familiar with dislocations.

ACKNOWLEDGMENT

The author wishes to express his appreciation to the United States Atomic Energy Commission for their support of his research conducted under the Inorganic Materials Research Division of the Lawrence Radiation Laboratory in Berkeley. He further wishes to thank Mr. Jim Mote for his advice and help in preparing this paper.

REFERENCES

1. L. Prandtl, Zeit. Angw. Math. Phys. 8, 85 (1928).
2. U. Dehlinger, Ann. Phys. 2, 749 (1929).
3. G. I. Taylor, Proc. Roy. Soc. A145, 362 (1934).
4. E. Orowan, Zeit. Phys. 89, 605, 614, 634, (1934).
5. M. Polanyi, Zeit. Phys. 89, 660 (1934).
6. V. Volterra, Paris, Ann. Éc. Norm. (3) 24, 401 (1907).
7. F. R. N. Nabarro, Advances in Phy. 1, 269 (1952).
8. J. D. Eshelby, Solid State Phys. 3, 79 (1956).
9. A. Seeger, Ency. of Phys. VII; Crystal Physics I, 383 (1956).
10. E. Kroner, Kontinuumstheorie der Versetzung und Eigenspannung, J. Springer (1958).
11. W. T. Read, Jr., Dislocations in Crystals, McGraw-Hill (1953).
12. A. Cottrell, Dislocations and Plastic Flow in Crystals, Oxford (1953).
13. J. Friedel, Les Dislocations, Gauthier-Villars (1956).
14. J. E. Dorn and J. D. Mote, "Physical Aspects of Creep" Proc. of the Third Symposium on Naval Structural Mechanics (1963).
15. D. Campbell, J. Simmons and J. E. Dorn, J. Appl. Mech. 83, 447 (1961).
16. G. Leibfried, Z. Phys. 127, 344 (1949).
17. H. Suzuki, Dislocations and Mechanical Properties of Crystals, McGraw-Hill 361 (1957).
18. A. Seeger, Phil. Mag. 1, 651 (1956).
19. A. Seeger, H. Donth and F. Pfaff, Disc. Faraday Soc. 23, 19 (1957).
20. Lothe and Hirth, Phys. Rev. 115, 543 (1959).
21. J. Friedel, Electron Microscopy and Strength of Crystals, Interscience 605 (1962).
22. J. Dorn and S. Rajnak, "Dislocations and Plastic Waves" to be published.
23. T. vonKarmann and P. Duwez, J. Appl. Phys. 21, 987 (1950).

24. G. I. Taylor, "Plastic Wave in Wire Extended By An Impact Load" Scientific Papers 1, Cambridge University Press (1958).

25. F. Frank and W. Read, Phys. Rev. 79, 722 (1950).

26. E. J. Sternglass and D. A. Stewart, J. Appl. Mech. 20, 427 (1953).

27. B. E. K. Alter and C. W. Curtis, J. Appl. Phys. 27, 1079 (1956).

28. C. Riparbelli, Proc. Soc. Exptl. Stress Analysis 14, 55-70 (1954).

29. J. Mote, K. Tanaka and J. Dorn, Trans. A. I. M. E. 221, 858 (1961).

30. J. E. Dorn and F. E. Hauser, University of California, Lawrence Radiation Laboratory Report # UCRL-10498.

31. J. E. Dorn and S. Rajnak, Univ. of Calif. Radiation Laboratory Report # UCRL-10789.

32. E. Howard, W. Barmore, J. Mote and J. E. Dorn, UCRL-10588 (to be published in AIME)

33. T. Larsen, S. Rajnak, F. E. Hauser and J. E. Dorn, "The Effect of Strain Rate and Temperature on the Yield Strength in Ag-Al Single Crystals" Rept. Contract UCX 2264, 2nd Tech. Rept. Series 174, Issue #2.